Research Article

iMedPub Journals
www.imedpub.com

Biochemistry & Molecular Biology Journal
ISSN 2471-8084

2021
Vol.7 No.1:3

Investigation of Promising Antiviral Candidate Molecules based on Algal Phlorotannin for the Prevention of COVID-19 Pandemic by *in silico* Studies

Khattab Al-Khafaji[1], Eyup Ilker Saygili[2,3], Tugba Taskin-Tok[1,4*], Zafer Cetin[5,6], Selin Sayın[7], Sinem Ugur[7], Merve Goksin Karaaslan[8], Oral Cenk Aktas[9], Haroon Khan[10] and Esra Küpeli Akkol[11*]

1 Department of Chemistry, Faculty of Arts and Sciences, Gaziantep University, Turkey
2 Department of Medical Biochemistry, School of Medicine, SANKO University, Turkey
3 Department of Molecular Medicine, Graduate Institute of Education, SANKO University, Turkey
4 Department of Bioinformatics and Computational Biology, Gaziantep University, Turkey
5 Department of Medical Biology, School of Medicine, SANKO University, Turkey
6 Department of Biological and Biomedical Sciences, Graduate Education Institute, SANKO University, Turkey
7 Department of Marine Technologies, Iskenderun Technical University, Turkey
8 Tashkent Vocational High School, Selçuk University, Turkey
9 Institute of Materials Science, Christian-Albrechts-University, Germany
10 Department of Pharmacy, Abdul Wali Khan University Mardan, Pakistan
11 Department of Pharmacognosy, Faculty of Pharmacy, Gazi University, Turkey

*Corresponding author: Tugba Taskin-Tok

ttaskin@gantep.edu.tr

Department of Chemistry, Faculty of Arts and Sciences, Gaziantep University, Turkey.

Tel: +903122023185

Abstract

Background: Coronavirus disease 19 (COVID-19) is a highly contagious and pathogenic viral infection. Research has been stepped up due to the lack of vaccine for this viral infection and no effective treatment against this new virus. In order to control the spread, the effectiveness of algal phlorotannin-derived natural molecules on COVID-19, which are easy to obtain, maintainable and have antiviral efficacy by focusing on the Spike (S) protein of the virus, was investigated by *in silico* methods.

Materials and methods: In this study, molecular docking was performed to highlight the emerging role of the top three molecules amongst the selected 11 compounds against SARS CoV-2-RBD/ACE2 and SARS CoV-2-Spike/TMPRSS2.

Results and Discussion: An *in silico* model of algal molecules interactivity on SARS CoV-2-RBD/ACE2 and SARS CoV-2-Spike/TMPRSS2 receptor was observed. Results suggested that based on *in silico* model, out of algal phlorotannin ligands, only a diecol showed good binding affinity toward SARS CoV-2-RBD/ACE2 interface, compared as remdesivir, chloroquine and hydroxychloroquine sulfate. Moreover within these potential molecules based phlorofucofuroeckol B can also be protector for only TMPRSS2.

Conclusion: In future, these results may be aid to direction of the design and development of potent drugs for COVID-19 treatment based on the severity of infection.

Keywords: ADMET; COVID-19; Spike (S) Protein; Algal phlorotannin; Molecular docking

Received: October 17, 2021; **Accepted:** January 23, 2021; **Published:** January 30, 2021

Introduction

Coronaviruses are enveloped RNA viruses that cause enteric, respiratory and central nervous system diseases in various animals and humans [1]. Coronavirus surface protein spikes (S) mediate entry into target cells by binding to a cellular receptor and then fusing the viral envelope with a host cell membrane [2]. SARS-CoV Spike protein (SARS-S) uses Angiotensin Converting Enzyme 2 (ACE2) as the host cell entry receptor [3,4]. Cleavage of the S protein by host cell proteases is essential for viral infectivity and responsible enzymes are potential targets for intervention [2]. The SARS-S enters angiotensin converting enzyme 2 (ACE2)

as the input receptor [3] and uses cellular Transmembrane Serine Protease 2 (TMPRSS2) for S protein preparation [5]. The SARS-S/ACE2 interface has been identified at the atomic level and the effectiveness of ACE2 use has been found to be the main determinant of SARS-CoV contamination [6].

Outbreaks from viral infectious diseases that have led to mass deaths throughout history show how they can threaten public health on a global scale. The current situation clearly shows that antiviral treatments that are effective against various virus strains should be developed immediately in the prevention and treatment of viruses. In the development of antiviral drug agent, molecules containing innovative functional groups are of great importance in the structure and effectiveness of drugs. The targeted properties of functional groups or systems and their effect on drug composition are very important [7]. At this point, the use of *in silico* methods has an important place in the development of antiviral drug agents' researches. In predicting the interactions of bioactive molecules and biological life systems with each other, the use of *in silico* methods saves considerable time, labor and cost.

In recent years, one of the alternative and sustainable ways of developing effective treatments against the related virus is the identification of potent agents. In this study, algae; it is a rich source of effective molecules such as phlorotannins, polysaccharides, pigments, glycolipids, catechin, terpenoids, polyhydroxyburates. Algae with their rich functional contents; It has an important potential with its biological activities such as anticancer, antimicrobial, anti-inflammatory and antiviral [8]. Phlorotannin is a class of polyphenol compounds produced by brown seaweed as secondary metabolites and biosynthesized through the acetate malonate pathway [9,10]. These compounds have attracted considerable research interest for their broad health benefits and potential uses in a range of therapeutics [11,12]. It has demonstrated that phlorotannins can have anti-diabetic, anti-cancer, anti-oxidation, antibacterial, radio protective and anti-HIV properties [13,14].

Based on this information, using *in silico* approaches within the scope of the study, the inhibitory effect of 11 compounds (Phloroglucinol, Eckol, Fucodiphloroechol-G, Phlorofucofuroeckol A, 7-Phloroeckol, Dieckol, 6,6'-Bieckol, Diphloroethohydroxycarmalol, 8,8'-Bieckol, Phlorofucofuroeckol B, Catechin) on the mechanism of action of SARS-CoV-2 was investigated. The potent molecules activity has been investigated and evaluated against the ACE2 and TMPRSS2 proteins to which SARS-CoV-2 binds.

Materials and Methods

Ligand-protein docking

The data set was composed of 11 compounds **(Table 1)** which were obtained from literature [15-22]. These natural compounds produce from algal organisms that shown antiviral activity were also remarked in introduction part of the study. Nowadays, *remdesivir* is the most hopeful SARS-CoV-2 drug, although Food and Drug Administration (FDA) has also confirmed the utilization

Citation: Al-Khafaji K, Saygili EI, Taskin-Tok T, Cetin Z, Sayın S, et al. (2021) Investigation of Promising Antiviral Candidate Molecules based on Algal Phlorotannin for the Prevention of COVID-19 Pandemic by *in silico* Studies. Biochem Mol Biol Vol.7 No.1:3

of *chloroquine* and *hydroxychloroquine* for emergency coronavirus treatment [23]. The following process, Discovery Studio (DS) 2019 (BIOVIA, 2016) was applied to arrange and to exert the docking calculations and also to define docking interactions of the selected compounds- SARS CoV-2-RBD/ACE2 and the selected compounds- SARS CoV-2-Spike/TMPRSS2 complexes. The crystal structures of target models, SARS CoV-2-RBD/ACE2 (PDB: 2AJF) was retrieved from protein data bank [24,25] and SARS CoV-2-Spike/TMPRSS2 was occurred based on Meng et al. study [26] by using Homology modelling for docking processes. The ligands, the selected eleven compounds were sketched and optimized in gas phase using the CHARMm force field [27] to prepare an ensemble of docking study with no atomic clashes in their geometries.

In addition, their conformational analyses were investigated by using DS 2019. On the other hand, both virus models were prepared using DS tools and minimized until the root mean square deviation (RMSD) reaches the lower value of 0.05 kcal/mol $Å^2$. The binding site tool in DS software and the related literatures information were used to detect binding site of the SARS CoV-2-RBD/ACE2 and SARS CoV-2-Spike/TMPRSS2 against the selected eleven natural structures.

Molecular docking is one of the most common procedures for generating ligand pose inside the pocket and determining the key residues which interact with ligand. Therefore, docking studies were executed using the docking software AutodockFR (ADFR) software [28] with the AutoGridFr (AGFR version 1.0) [29,30] which is responsible for building configuration file which contains the data for running controlled flexible docking by detecting the residues of the complex's binding site. This enables ligands reaches buried grooves after running docking calculations by running of ADFR with presumptive parameters for all complexes [31]. The docking results for each complex was ranked according to the binding energy, root mean square deviation (RMSD) and interaction types.

In silico ADMET prediction

As known that the effectiveness and safety of a potential drug agent depends essentially on the biotransformations that occur in the organism. Therefore, drug-likeness properties including Lipinski [32] and Veber [33] tests for the selected compounds and *remdesivir, chloroquine* and *hydroxychloroquine sulfate* are effective drugs against SARS CoV-2 as positive controls were used and filtered by using DS 2019 [34]. In the following step, ADMET (Absorption, Distribution, Metabolism, Excretion and Toxicity) prediction was applied for the same compounds with help of ADMET subprotocol of Discovery Studio 2019 software using the prediction model by Egan et al. [35,36]. Water solubility (log S), $CaCO_2$ cell permeability for the prediction of oral drug absorption,

Table 1 Chemical structures of 11 compounds produce from algal organisms.

Name	Herbal name	Chemical Structure, SMILES	Molecular Formula
1	Phloroglucinol	Oc1cc(O)cc(O)c1	$C_6H_6O_3$
2	Eckol	Oc1cc(O)cc(Oc2c(O)cc(O)c3Oc4cc(O)cc(O)c4Oc23)c1	$C_{18}H_{12}O_9$
3	Fucodiphloroechol – G	Oc1cc(O)c(Oc2cc(O)cc(O)c2Oc3cc(O)cc(O)c3c4c(O)cc(O)cc4O)c(O)c1	$C_{24}H_{18}O_{12}$
4	Phlorofucofuroeckol A	Oc1cc(O)cc(Oc2c(O)cc(O)c3Oc4c(Oc23)c(O)cc5oc6c(Oc7cc(O)cc(O)c7)c(O)cc(O)c6c45)c1	$C_{30}H_{18}O_{14}$
5	7-Phloroeckol	Oc1cc(O)c(Oc2cc(O)c3Oc4c(Oc5cc(O)cc(O)c5)c(O)cc(O)c4Oc3c2)c(O)c1	$C_{24}H_{16}O_{12}$
6	Dieckol	Oc1cc(O)cc(Oc2c(O)cc(O)c3Oc4cc(Oc5c(O)cc(Oc6c(O)cc(O)c7Oc8cc(O)cc(O)c8Oc67)cc5O)cc(O)c4Oc23)c1	$C_{36}H_{22}O_{18}$
7	6,6-Bieckol	Oc1cc(O)cc(Oc2c(O)cc(O)c3Oc4c(Oc23)c(O)cc(O)c4c5c(O)cc(O)c6Oc7c(Oc8cc(O)cc(O)c8)c(O)cc(O)c7Oc56)c1	$C_{36}H_{22}O_{18}$
8	Diphloroethohydroxycarmalol	Oc1cc(O)c(Oc2cc3Oc4c(O)c(Oc5cc(O)cc(O)c5)c(O)c(O)c4Oc3c(O)c2O)c(O)c1	$C_{24}H_{16}O_{14}$
9	8,8-Bieckol	Oc1cc(O)cc(Oc2c(O)cc(O)c3Oc4cc(O)c(c(O)c4Oc23)c5c(O)cc6Oc7c(O)cc(O)c(Oc8cc(O)cc(O)c8)c7Oc6c5O)c1	$C_{36}H_{22}O_{18}$
10	Phlorofucofuroeckol B	Oc1cc(O)cc(Oc2c(O)cc(O)c3Oc4cc5oc6c(Oc7cc(O)cc(O)c7)c(O)cc(O)c6c5c(O)c4Oc23)c1	$C_{30}H_{18}O_{14}$
11	Catechin	O[C@H]1Cc2c(O)cc(O)cc2O[C@@H]1c3ccc(O)c(O)c3	$C_{15}H_{14}O_6$
*Remdesivir	Remdesivir	CCC(CC)COC(=O)[C@H](C)N[P@@](=O)(OC[C@H]1O[C@](C#N)([C@H](O)[C@@H]1O)c2ccc3c(N)ncnn23)Oc4ccccc4	$C_{27}H_{35}N_6O_8P$
*Chloroquine	Chloroquine	CCN(CC)CCC[C@@H](C)Nc1ccnc2cc(Cl)ccc12	$C_{18}H_{26}ClN_3$
*Hydroxychloroquine sulfate	Hydroxychloroquine sulfate	CCN(CCO)CCC[C@H](C)Nc1ccnc2cc(Cl)ccc12	$C_{18}H_{28}ClN_3O_5S$
*Remdesivir, chloroquine and hydroxychloroquine are potent drugs against SARS CoV-2 as positive controls.			

Human ether-a-go-go related gene (hERG) inhibition and toxicity descriptors (AMES toxicity, Hepatotoxicity and Skin sensitization) were calculated. In summary, it was applied to allow a deeper insight into applicability of the selected compounds to be safe for potential drug development against SARS-CoV- 2.

Results

Molecular docking study

For effective docking process, a potential drug agent should fit the active site of an individual target. That means non-bonding interactions including hydrogen bond, electrostatic and hydrophobic have a tremendous impact on docking results. The binding energies of the molecules shape complementarity are also an indispensable condition. The key is to define the correct binding mode with most stable interactions. Binding energy values of the selected ligands represent their affinity to form durable interactions inside the pockets of both targets. A low binding energy value signifies a strong binding and vice versa [37]. Based on these information, out of 11 ligands, only a 33% showed good binding affinity toward SARS CoV-2-RBD/ACE2 interface, compared as remdesivir, chloroquine and hydroxychloroquine sulfate. However, this ratio raised to 42% when 11 ligands docked to SARS CoV-2-Spike/TMPRSS2 interface as presented in the **Table 2.** What is intriguing about the data in this table is that both of Dieckol (**6**) and Phlorofucofuroeckol B (**10**) are ranked of top three against both targets. We attended to explore the top three compounds and their interactions with each of the selected complex. The top one is Dieckol (**6**) when it binds to SARS CoV-2-RBD/ACE2. The interactions of Dieckol (**6**) with the lowest binding affinity (-7.406 kcal/mol) as displayed in **Table 3** which forms five hydrogen bonds with Gly354, Ala386 of ACE2 and six hydrogen bonds with Lys390, Gln396, Tyr491, Asp393 residues of SARS CoV-2-RBD protein. Besides hydrogen bond, there are five electrostatic interactions with Lys390, Asp392 and Asp393 of ACE2 and eight hydrophobic interactions with four residues of ACE2 protein (Phe356, Met383, Ala386 and Ala387) and also two residues of SARS-CoV-2-RBD protein (Tyr440 and Val404) **(Figure 1).** While Dieckol comes in second rank of binding affinity (-9.039 kcal/mol) to bind with SARS CoV-2-Spike/TMPRSS2. Where it formed three hydrogen bonds and five hydrophobic interactions as shown in **Figure 2,** where Dieckol (**6**) interacted in the interface of SARS CoV-2-Spike/TMPRSS2, through forming two hydrogen bonds with both Phe194 and Pro288 and five vander Waal interactions with Pro288, Phe357 and Pro354 of TMPRSS2 protein. Besides, it forms one hydrogen bond through Asp820 of SARS CoV-2-Spike. Another significant finding is related to 8,8-Bieckol (**9**) which ranked second when it bound to SARS CoV-2-RBD/ACE2 complex with the binding affinity of – 7.253 kcal/mol. First, 8,8-Bieckol (**9**) interacted with SARS CoV-2-RBD/ACE2 interface through two conventional hydrogen bonds all of them with ACE2 protein residues (Arg393) and two carbon-hydrogen bonds with Thr324 and Gly354 as presented in **Figure 1**. Furthermore, the residues (Ala386 and Ala387) of ACE2 form three hydrophobic interactions with 8,8-Bieckol (**9**). Despite these interactions, SARS CoV-2-RBD interacted with 8,8-Bieckol (**9**) through nine hydrogen bonds (Arg395, Gly490, Asp392, Gly391 and Gly490) and three electrostatic interactions through Arg395 and Asp392 of SARS CoV-2-RBD, and also one hydrophobic interaction with Ile489 residue in the related protein, **(Figure 1).**

Table 2 ADMET analysis of 11 compounds and positive controls* (Remdesivir, chloroquine and hydroxychloroquine sulfate) for SARS CoV-2-RBD/ACE2 and SARS CoV-2-Spike/TMPRSS2).

Name	Donor HB	Accpt HB	logS	$CaCO_2$	loghERG	AMES toxicity	Hepatotoxicity	Skin sensitization
Range	2/20	2/20	-6.5/0.5	<25 poor, >500 great	<-5		True: Toxic/False: Non-Toxic	
1	3	2	-0.384	269.113	-3.257	Non-Mutagen	False	Strong
2	6	6	-2.619	17.844	-5.201	Non-Mutagen	False	Strong
3	10	9	-2.883	0.919	-6.411	Non-Mutagen	False	Strong
4	9	9	-4.279	1.791	-6.85	Mutagen	False	None
5	8	8	-3.484	2.728	-6.292	Non-Mutagen	False	Strong
6	11	12	-5.313	0.162	-7.929	Non-Mutagen	False	Strong
7	12	12	-3.89	0.344	-6.761	Non-Mutagen	False	Strong
8	10	10	-3.265	0.327	-6.506	Non-Mutagen	False	Strong
9	12	12	-3.993	0.219	-6.805	Non-Mutagen	False	Strong
10	9	9	-4.325	1.539	-6.913	Mutagen	False	None
11	5	5	-2.591	57.005	-4.784	Non-Mutagen	False	Strong
*Remdesivir	5	17	-5.107	33.727	-6.788	Non-Mutagen	True	None
*Chloroquine	2	6	-3.198	438.709	-5.941	Mutagen	True	None
*Hydroxychloroquine	1	4	-3.82	1403.192	-5.766	Mutagen	True	None

Table 3 Docking Results of 11 compounds toward SARS CoV-2-RBD/ACE2 and SARS CoV-2-Spike/TMPRSS2 complex.

Compound Name	SARS CoV-2-RBD/ACE2		SARS CoV-2-Spike/TMPRSS2	
	Binding energy (kcal/mol)	RMSD (Å)	Binding energy (kcal/mol)	RMSD (Å)
1	-4.272	0.859	-4.952	0.474
2	-5.412	1.223	-7.257	1.173
3	-6.039	2.041	-7.325	3.791
4	-6.672	2.302	-7.942	2.125
5	-6.229	1.290	-8.283	1.512
6	-7.406	2.021	-9.039	3.679
7	-6.651	1.516	-9.177	1.058
8	-6.188	3.532	-8.313	3.601
9	-7.253	2.786	-8.285	2.260
10	-6.939	1.955	-8.515	1.801
11	-5.196	1.291	-6.240	1.619
*Remdesivir	-6.537	3.562	-8.011	2.269
*Chloroquine	-5.234	2.310	-5.738	1.429
*Hydroxychloroquine sulfate	-5.185	1.873	-5.920	2.235
*Remdesivir, chloroquine and hydroxychloroquine sulfate are potent drugs against SARS CoV-2 as positive controls.				

Turning now to another promising compound that is 6,6-Bieckol (**7**) which has lowest binding score (-9.177 kcal//mol), with four hydrogen bonds with when it binds to SARS CoV-2-Spike/TMPRSS2. Where it forms four hydrogen bonds with SARS CoV-2 Spike protein residues (Thr827, Val826 and Asn824) and four hydrophobic interactions with TMPRSS2 residues (Pro288, Phe194 and Pro354) as shown in **Figure 2**. On the other hand, phlorofucofuroeckol B (**10**) ranked as third when it screened against SARS CoV-2-RBD/ACE2 and SARS CoV-2-Spike/TMPRSS2 of binding affinity (-6.939 and -8.515 kcal/mol), respectively. This compound interacted three hydrogen bonds with the residues of SARS CoV-2-RBD (Lys390, Gln396 and Tyr491) and five electrostatic interactions with Lys390 and Asp393 residues and also three hydrophobic interactions with Tyr440, Tyr491 and Val404 of SARS CoV-2-RBD. In addition, it interacted through forming one hydrogen bond (Glu37) and three hydrophobic interactions with ACE2 protein residues (Ala386), **Figure 1**. The compound, phlorofucofuroeckol B (**10**) has a good ability to establish four conventional hydrogen bonds with TMPRSS2 residues (Phe357, Thr287, Glu289, Cys241) and one carbon-hydrogen bonds with TMPRSS2 residues (Pro288) as shown in **Figure 2**. Also, it interacted through forming two electrostatic interactions with Arg240 of TMPRSS2 and five hydrophobic interactions with TMPRSS2 residues (Phe357, Ala243, Pro288, Pro354 and Ala243). This indicative interaction tells us that phlorofucofuroeckol B (**10**) prefers to bind with TMPRSS2 protein.

Besides these docking calculations, the same docking processes were also applied by using three potent drugs against SARS CoV-2 as three positive controls: *remdesivir*, is noted for its capacity to reduce the viral load in the lung tissue of mice infected with the MERS-CoV virus, improving lung function and damage to lung tissue [38] and, chloroquine and hydroxychloroquine sulfate

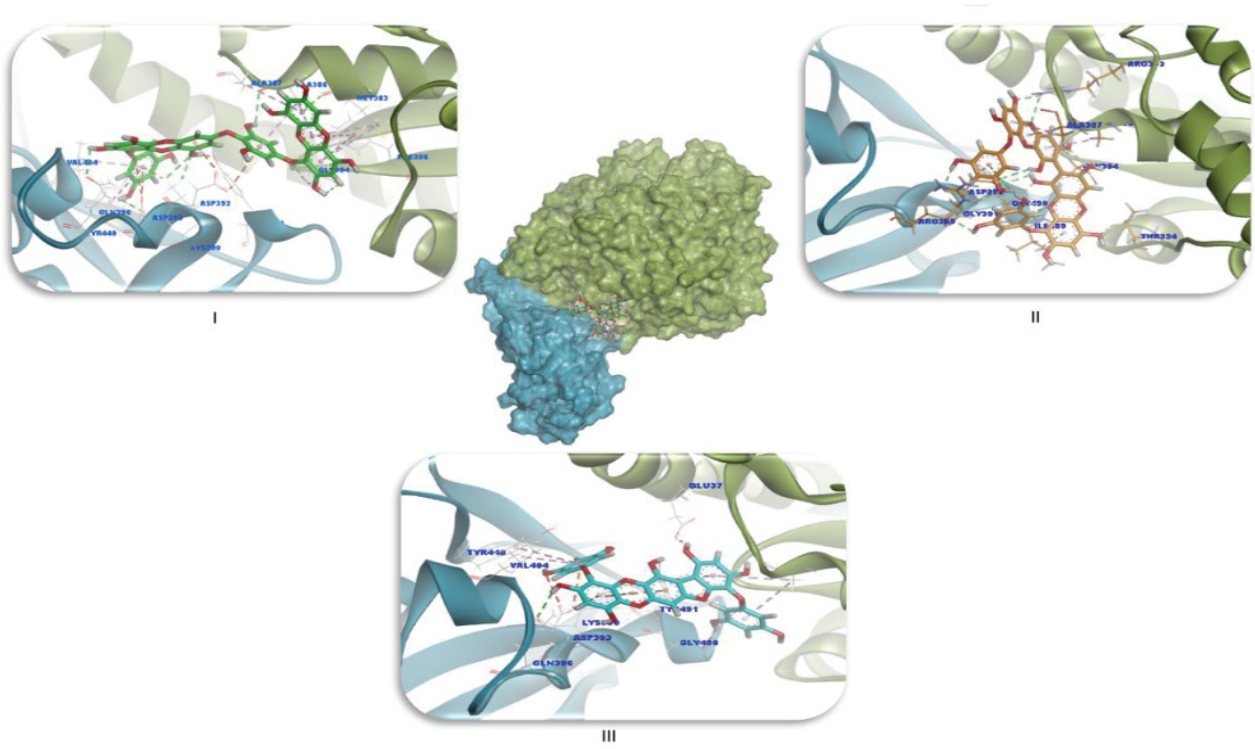

Figure 1 Docking results of I-Dieckol (**6,** green), II-8,8-Bieckol (**9,** orange) and III-Phlorofucofuroeckol B (**10,** magenta), and their poses in the SARS CoV-2-RBD /ACE2 (blue/dark green) interface.

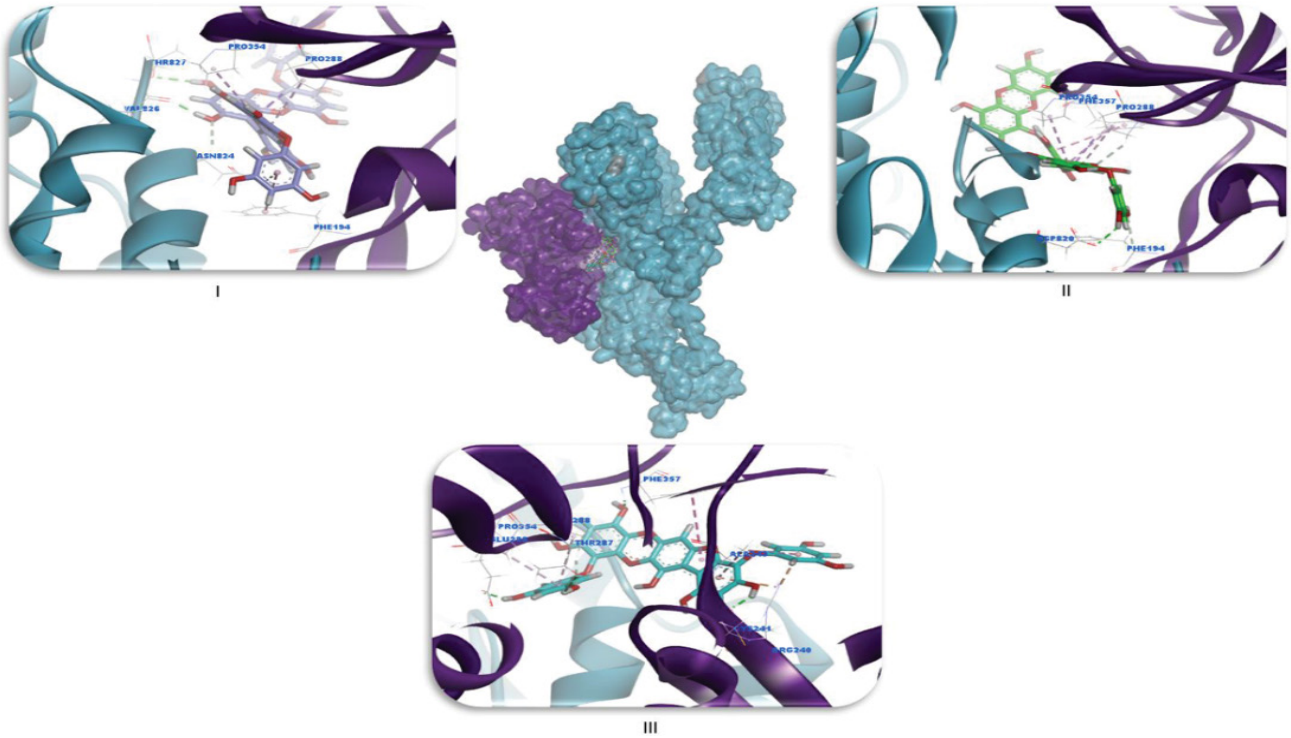

Figure 2 Docking results of I-6,6-Bieckol (**7,** light violet), II-Dieckol (**6,** green), and III-Phlorofucofuroeckol B (**10,** magenta), and their poses in the SARS CoV-2-Spike/TMPRSS2 (blue/violet) interface.

are further used anti-malarial drugs recommended by the FDA against SARS CoV-2 [23]. **(Figure 3 and Table 4**). Compared with control compounds and also with the orientation and conformation of the studied top three compounds at the SARS CoV-2-RBD/ACE2 and SARS CoV-2-Spike/TMPRSS2 pockets allow more potent binding **(Table 3)** and efficient interactions **(Figure 1 and Figure 2).** In summary, it was revealed that dieckol (**6**) and phlorofucofuroeckol B (**10**) prefer to bind with ACE2 and TMPRSS2 receptors more than SARS CoV-2 Spike and SARS CoV-2-RBD proteins. So that the compound (dieckol) can be protector for the cell receptors (ACE2 and TMPRSS2). Phlorofucofuroeckol B can also be protector for only TMPRSS2.

In silico ADMET analysis

ADMET properties were assessed by ADMET subprotocol of Discovery Studio 2019 software. It compiles pharmacokinetic properties for selected ligands along with control compounds (remdesivir, chloroquine and hydroxychloroquine sulfate) in **Table 2.** Basically, the poor solubility associates with poor absorption. So the water solubility (log S) of a compound significantly influences its absorption features. The predicted log S values of all top four compounds [dieckol (**6**), 6,6-Bieckol (**7**), 8,8-Bieckol (**9**) and phlorofucofuroeckol B (**10**)] were within the tolerable limit. Donor and acceptor of hydrogen bonding are essentials of Lipinski rule and all the ligands were displayed within the acceptable range of drug-likeliness. $CaCO_2$ intestinal cell line permeability is measured in nm/sec and is meaningful for intestinal absorption. Its value was lower than the limited value for among the top four tested ligands. The log hERG (log IC_{50}) values for dieckol (**6**), phlorofucofuroeckol B (**10**), 8,8-Bieckol (**9**) and 6,6-Bieckol (**7**) display the finest results among eleven ligands. The negative value of log hERG shows that the lower the value of log hERG, the lesser is the blockage of K+ ion channels [37]. The results of *in silico* ADMET studies implied that dieckol (**6**) and phlorofucofuroeckol B (**10**) exhibited fine pharmacokinetic profile. Further, the predicted toxicity data (AMES toxicity, hepatotoxicity, skin sensitization values) reveal that the lead compounds have no toxicity and present demanded range**.** Henceforth they could be foreseen as safe for drug development against human epidemics of SARS-CoV-2.

Discussion

The mechanisms of antiviral actions of algal bioactive compounds include direct virucidal action, inhibition of viral attachment to host cells, inhibition of virus internalization and uncoating in the target cell, inhibition of viral transcription and replication and improvement of antiviral immune responses in host cells [39].

Several reports have done that the routes of SARS CoV-2 protein targets, structures and models (Main Protease, Papain-like protease, Spike RBD, Spike monomer and trimer etc) administration can affect the nature of the treatment toward SARS CoV-2. In the meantime, it is present different ligands having antibody, peptide and small molecules are used to prevent or stop the activities of the disease. The all documents such as targets, structure, models, therapeutics... etc. are present in website, data hub or server systems [40-43].

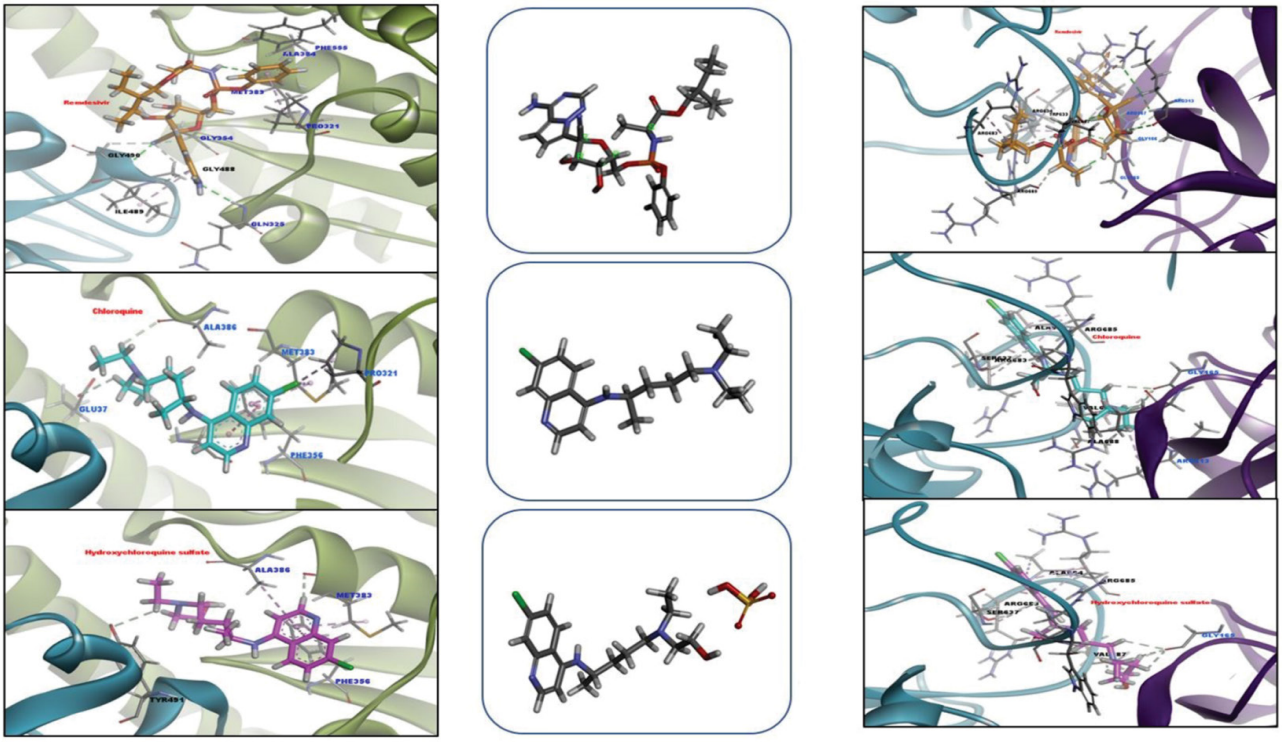

Figure 3 3D docking poses of remdesivir, chloroquine and hydroxychloroquine sulfate within the binding pocket of SARS CoV-2-RBD /ACE2 (left side) and SARS CoV-2-Spike /TMPRSS2 (right side), respectively.

Table 4 Interactions types and distances of three positive controls (Remdesivir, chloroquine and hydroxychloroquine sulfate) and the three better compounds [Diekcol (**6**), 8,8-Bieckol (**9**) and Phlorofucofuroeckol B (**10**)] with SARS CoV-2-RBD/ACE2 and [6,6-Bieckol (**7**), Diekcol (**6**) and Phlorofucofuroeckol B (**10**)] with SARS CoV-2-Spike/TMPRSS2, respectively.

SARS CoV-2-RBD/ACE2					
Interactions-Remdesivir	**Distance Å**	**Bonding**	**Bonding Types**	**Target**	**Ligand**
A: GLN325: HN - Remdesivir: N30	2.7938	Hydrogen Bond	Conventional Hydrogen Bond	A: GLN325: HN	Remdesivir: N30
E: GLY490: HN - Remdesivir: N26	2.4758	Hydrogen Bond	Conventional Hydrogen Bond	E: GLY490: HN	Remdesivir: N26
Remdesivir: H47 - A: MET383: O	2.9175	Hydrogen Bond	Conventional Hydrogen Bond	A: MET383: O	Remdesivir: H47
A: GLY354: HA1 - Remdesivir: N26	2.5265	Hydrogen Bond	Carbon Hydrogen Bond	A: GLY354: HA1	Remdesivir: N26
E: GLY488: HA1 - Remdesivir: N26	2.6010	Hydrogen Bond	Carbon Hydrogen Bond	E: GLY488: HA1	Remdesivir: N26
E: GLY490: HA1 - Remdesivir: N26	3.0246	Hydrogen Bond	Carbon Hydrogen Bond	E: GLY490: HA1	Remdesivir: N26
E: ILE489: HN - Remdesivir	3.0680	Hydrogen Bond	Pi-Donor Hydrogen Bond	E: ILE489: HN	Remdesivir
Remdesivir - A: PRO321	4.2456	Hydrophobic	Pi-Alkyl	A: PRO321	Remdesivir
Remdesivir - A: ALA384	4.7492	Hydrophobic	Pi-Alkyl	A: ALA384	Remdesivir
Remdesivir - E: ILE489	4.7178	Hydrophobic	Pi-Alkyl	E: ILE489	Remdesivir
Interactions-Chloroquine	**Distance Å**	**Bonding**	**Bonding Types**	**Target**	**Ligand**
Chloroquine: H40 - A: ALA386: O	2.8499	Hydrogen Bond	Carbon Hydrogen Bond	A: ALA386: O	Chloroquine: H40
Chloroquine: H42 - A: GLU37: OE1	2.8475	Hydrogen Bond	Carbon Hydrogen Bond	A: GLU37: OE1	Chloroquine: H42
Chloroquine-A: PHE356	5.7629	Hydrophobic	Pi-Pi T-shaped	A: PHE356	Chloroquine
Chloroquine- A: PHE356	5.1758	Hydrophobic	Pi-Pi T-shaped	A: PHE356	Chloroquine
Chloroquine: CL20 - A: PRO321	4.0220	Hydrophobic	Alkyl	A: PRO321	Chloroquine: CL20
Chloroquine: CL20 - A: MET383	3.5397	Hydrophobic	Alkyl	A: MET383	Chloroquine: CL20
Chloroquine - A: MET383	4.7875	Hydrophobic	Pi-Alkyl	A: MET383	Chloroquine
Interactions-Hydroxychloroquine sulfate	**Distance Å**	**Bonding**	**Bonding Types**	**Target**	**Ligand**
Hydroxychloroquine sulfate: H27 - E: TYR491: OH	3.0534	Hydrogen Bond	Carbon Hydrogen Bond	E: TYR491: OH	Hydroxychloroquine sulfate: H27
Hydroxychloroquine sulfate: H43 - A: MET383: O	2.6589	Hydrogen Bond	Carbon Hydrogen Bond	A: MET383: O	Hydroxychloroquine sulfate: H43
Hydroxychloroquine sulfate - A: PHE356	5.1956	Hydrophobic	Pi-Pi T-shaped	A: PHE356	Hydroxychloroquine sulfate
Hydroxychloroquine sulfate - A: MET383	4.9256	Hydrophobic	Pi-Alkyl	A: MET383	Hydroxychloroquine sulfate
Hydroxychloroquine sulfate - A: ALA386	5.4130	Hydrophobic	Pi-Alkyl	A: ALA386	Hydroxychloroquine sulfate
Interactions-Dieckol	**Distance Å**	**Bonding**	**Bonding Types**	**Target**	**Ligand**
E: LYS390: HZ2 - Dieckol: O45	2.4977	Hydrogen Bond	Conventional Hydrogen Bond	E: LYS390: HZ2	Dieckol: O45
E: LYS390: HZ3 - Dieckol: O45	2.9174	Hydrogen Bond	Conventional Hydrogen Bond	E: LYS390: HZ3	Dieckol: O45
Dieckol: H59 - A: GLY354: O	2.9561	Hydrogen Bond	Conventional Hydrogen Bond	A: GLY354: O	Dieckol: H59
Dieckol: H64 - A: ALA386: O	2.8949	Hydrogen Bond	Conventional Hydrogen Bond	A: ALA386: O	Dieckol: H64
Dieckol: H70 - E: GLN396: OE1	2.8332	Hydrogen Bond	Conventional Hydrogen Bond	E: GLN396: OE1	Dieckol: H70
Dieckol: H71 - E: TYR491: OH	1.9152	Hydrogen Bond	Conventional Hydrogen Bond	E: TYR491: OH	Dieckol: H71
Dieckol: H75 - E: ASP393: OD2	2.7816	Hydrogen Bond	Conventional Hydrogen Bond	E: ASP393: OD2	Dieckol: H75
A: GLY354: HA1 - Dieckol: O16	2.5775	Hydrogen Bond	Carbon Hydrogen Bond	A: GLY354: HA1	Dieckol: O16
A: GLY354: HA1 - Dieckol: O19	2.9464	Hydrogen Bond	Carbon Hydrogen Bond	A: GLY354: HA1	Dieckol: O19
A: GLY354: HA2 - Dieckol: O19	3.0035	Hydrogen Bond	Carbon Hydrogen Bond	A: GLY354: HA2	Dieckol: O19

SARS CoV-2-RBD/ACE2					
Interactions-Remdesivir	**Distance Å**	**Bonding**	**Bonding Types**	**Target**	**Ligand**
E: LYS390: HZ3 - Dieckol	2.3468	Hydrogen Bond;Electrostatic	Pi-Cation;Pi-Donor Hydrogen Bond	E: LYS390: HZ3	Dieckol
E: ASP392: OD1 - Dieckol	4.4474	Electrostatic	Pi-Anion	E: ASP392: OD1	Dieckol
E: ASP392: OD2 - Dieckol	3.3188	Electrostatic	Pi-Anion	E: ASP392: OD2	Dieckol
E: ASP393: OD1 - Dieckol	4.5729	Electrostatic	Pi-Anion	E: ASP393: OD1	Dieckol
E: ASP393: OD1 - Dieckol	3.9606	Electrostatic	Pi-Anion	E: ASP393: OD1	Dieckol
E: TYR440 - Dieckol	5.2778	Hydrophobic	Pi-Pi Stacked	E: TYR440	Dieckol
A: PHE356 - Dieckol	5.8437	Hydrophobic	Pi-Pi T-shaped	A: PHE356	Dieckol
A: PHE356 - Dieckol	5.2454	Hydrophobic	Pi-Pi T-shaped	A: PHE356	Dieckol
Dieckol - A: MET383	5.1850	Hydrophobic	Pi-Alkyl	A: MET383	Dieckol
Dieckol - A: MET383	5.3465	Hydrophobic	Pi-Alkyl	A: MET383	Dieckol
Dieckol - A: ALA386	4.6125	Hydrophobic	Pi-Alkyl	A: ALA386	Dieckol
Dieckol - A: ALA386	4.5717	Hydrophobic	Pi-Alkyl	A: ALA386	Dieckol
Dieckol - A: ALA387	5.4374	Hydrophobic	Pi-Alkyl	A: ALA387	Dieckol
Dieckol - A: ALA386	4.9676	Hydrophobic	Pi-Alkyl	A: ALA386	Dieckol
Dieckol - E: VAL404	4.9313	Hydrophobic	Pi-Alkyl	E: VAL404	Dieckol
Interactions-8,8-Bieckol	**Distance Å**	**Bonding**	**Bonding Types**	**Target**	**Ligand**
A: ARG393: HH21 - 8,8-Bieckol: O24	2.9012	Hydrogen Bond	Conventional Hydrogen Bond	A: ARG393: HH21	8,8-Bieckol: O24
A: ARG393: HH21 - 8,8-Bieckol: O34	2.2271	Hydrogen Bond	Conventional Hydrogen Bond	A: ARG393: HH21	8,8-Bieckol: O34
E: ARG395: HE - 8,8-Bieckol: O45	2.4215	Hydrogen Bond	Conventional Hydrogen Bond	E: ARG395: HE	8,8-Bieckol: O45
E: GLY490: HN - 8,8-Bieckol: O3	2.2512	Hydrogen Bond	Conventional Hydrogen Bond	E: GLY490: HN	8,8-Bieckol: O3
8,8-Bieckol: H57 - E: ASP392: OD1	2.6917	Hydrogen Bond	Conventional Hydrogen Bond	E: ASP392: OD1	8,8-Bieckol: H57
8,8-Bieckol: H66 - E: ASP392: OD2	2.6695	Hydrogen Bond	Conventional Hydrogen Bond	E: ASP392: OD2	8,8-Bieckol: H66
8,8-Bieckol: H70 - E: ASP392: O	2.2937	Hydrogen Bond	Conventional Hydrogen Bond	E: ASP392: O	8,8-Bieckol: H70
8,8-Bieckol: H75 - E: ASP392: OD2	2.4938	Hydrogen Bond	Conventional Hydrogen Bond	E: ASP392: OD2	8,8-Bieckol: H75
8,8-Bieckol: H76 - E: GLY391: O	2.6050	Hydrogen Bond	Conventional Hydrogen Bond	E: GLY391: O	8,8-Bieckol: H76
A: THR324: HB - 8,8-Bieckol: O17	2.7874	Hydrogen Bond	Carbon Hydrogen Bond	A: THR324: HB	8,8-Bieckol: O17
A: GLY354: HA2 - 8,8-Bieckol: O35	2.6753	Hydrogen Bond	Carbon Hydrogen Bond	A: GLY354: HA2	8,8-Bieckol: O35
E: GLY490: HA1 - 8,8-Bieckol: O3	2.9183	Hydrogen Bond	Carbon Hydrogen Bond	E: GLY490: HA1	8,8-Bieckol: O3
E: GLY490: HA1 - 8,8-Bieckol: O15	2.5716	Hydrogen Bond	Carbon Hydrogen Bond	E: GLY490: HA1	8,8-Bieckol: O15
E: ARG395: NH2 - 8,8-Bieckol	4.0496	Electrostatic	Pi-Cation	E: ARG395: NH2	8,8-Bieckol
E: ASP392: OD1 - 8,8-Bieckol	3.7168	Electrostatic	Pi-Anion	E: ASP392: OD1	8,8-Bieckol
E: ASP392: OD2 - 8,8-Bieckol	3.3036	Electrostatic	Pi-Anion	E: ASP392: OD2	8,8-Bieckol
A: ALA387: HA - 8,8-Bieckol	2.6522	Hydrophobic	Pi-Sigma	A: ALA387: HA	8,8-Bieckol
8,8-Bieckol - E: ILE489	4.7007	Hydrophobic	Pi-Alkyl	E: ILE489	8,8-Bieckol
8,8-Bieckol - A: ALA386	4.3628	Hydrophobic	Pi-Alkyl	A: ALA386	8,8-Bieckol
8,8-Bieckol - A: ALA387	4.7288	Hydrophobic	Pi-Alkyl	A: ALA387	8,8-Bieckol
Interactions-Phlorofucofuroeckol B	**Distance Å**	**Bonding**	**Bonding Types**	**Target**	**Ligand**
Phlorofucofuroeckol B: H58 - A: GLU37: OE1	2.0637	Hydrogen Bond	Conventional Hydrogen Bond	A: GLU37: OE1	Phlorofucofuroeckol B: H58
Phlorofucofuroeckol B: H60 - E: GLN396: OE1	2.7084	Hydrogen Bond	Conventional Hydrogen Bond	E: GLN396: OE1	Phlorofucofuroeckol B: H60
Phlorofucofuroeckol B: H62 - E: TYR491: OH	2.6045	Hydrogen Bond	Conventional Hydrogen Bond	E: TYR491: OH	Phlorofucofuroeckol B: H62
E: LYS390: NZ - Phlorofucofuroeckol B	4.9696	Electrostatic	Pi-Cation	E: LYS390: NZ	Phlorofucofuroeckol B
E: LYS390: NZ - Phlorofucofuroeckol B	4.6371	Electrostatic	Pi-Cation	E: LYS390: NZ	Phlorofucofuroeckol B

SARS CoV-2-RBD/ACE2					
Interactions-Remdesivir	Distance Å	Bonding	Bonding Types	Target	Ligand
E: LYS390: HZ3 - Phlorofucofuroeckol B	2.6050	Hydrogen Bond;Electrostatic	Pi-Cation;Pi-Donor Hydrogen Bond	E: LYS390: HZ3	Phlorofucofuroeckol B
E: ASP393: OD1 - Phlorofucofuroeckol B	4.0933	Electrostatic	Pi-Anion	E: ASP393: OD1	Phlorofucofuroeckol B
E: ASP393: OD1 - Phlorofucofuroeckol B	4.6346	Electrostatic	Pi-Anion	E: ASP393: OD1	Phlorofucofuroeckol B
E: TYR440 - Phlorofucofuroeckol B	5.2464	Hydrophobic	Pi-Pi Stacked	E: TYR440	Phlorofucofuroeckol B
E: TYR491 - Phlorofucofuroeckol B	5.2086	Hydrophobic	Pi-Pi T-shaped	E: TYR491	Phlorofucofuroeckol B
Phlorofucofuroeckol B - A: ALA386	5.2691	Hydrophobic	Pi-Alkyl	A: ALA386	Phlorofucofuroeckol B
Phlorofucofuroeckol B - E: VAL404	4.6856	Hydrophobic	Pi-Alkyl	E: VAL404	Phlorofucofuroeckol B
Phlorofucofuroeckol B - A: ALA386	5.1446	Hydrophobic	Pi-Alkyl	A: ALA386	Phlorofucofuroeckol B

For example, using the homology modeling models of the Spike glycoprotein and SARS CoV-2 protease $3CL^{PRO}$ have developed and docking analysis were performed by Hall and Ji 2020, utilizing previously known approved compounds. They suggested several potent inhibitors on the $3CL^{PRO}$ main proteinase activity including; Zanamivir approved for the treatment of influenza A and B viruses, Indinavir and Saquinavir for treatment of HIV, Remdesivir at experimental stages that has shown clinical activity against the SARS-coronavirus, Ebola virus, and possibly the SARS CoV-2, Flavin Adenine Dinucleotide (FAD) and Coenzyme A [44]. It is also reported that, the aflavin was able to dock in the catalytic pocket near the active site of RdRp in SARS CoV-2, SARS CoV, and MERS CoV in the two different molecular docking methods [45].

Besides these, the study [46] estimates antagonists of SARS CoV-2 Mpro, SARS CoV-3CLpro, ACE2 Receptor and NSP12 RNA Polymerase against COVID-19, based on already approved 28 drugs, using last disease mechanisms discoveries. Further, it exhibited that hydroxychloroquine, chloroquine were not showed effective, as monotherapies, against COVID-19 or lung cell receptors. Herein, this fact was once again revealed at the molecular level, using silico methods, and the results were validated that chloroquine is not a suitable and effective drug for the treatment of COVID-19 in this article.

Based on these results, molecular docking for our study was performed to explain the effect of the top three molecules amongst the selected 11 compounds against both targets;SARS CoV-2-RBD/ACE2 and SARS CoV-2-Spike/TMPRSS2. These targets play important roles in prevent and transmission pathways of the related virus and considered as therapeutic targets for disease treatment. Dieckol (**6**) efficiently docked to the hydrophobic groove of SARS CoV-2-RBD/ACE2. Following, 8,8-Bieckol (**9**) and Phlorofucofuroeckol B (**10**) interact with the same target. Dieckol (**6**) compound has similar behavior as 8,8-Bieckol (**9**). Furthermore, these compounds display good activity with SARS CoV-2-RBD/ACE2 due to hydroxyl groups in their frame structures. Dieckol and diphlorethohydroxycarmalol phlorotanins isolated from *Ecklonia cava* Kjelman strongly inhibited HIV-1 Reverse Transcriptase (RT) activity and moderately inhibited HIV-1 protease activity. Dieckol inhibited the syncytium formation and penetration of HIV into cells, viral replication, and virus induced lytic effects [47].

For another target, (SARS CoV-2-Spike/TMPRSS2) 6,6-Bieckol (**7**) bounds in the position of two proteins interface with the lowest binding energy (-9.177 kcal//mol) in other compounds. In the meantime, among the polyphenolic compounds 6,6-Bieckol isolated from *Ecklonia cava* was found to be inhibitory effect on HIV-1 induced syncytia formation, cell–virus and cell–cell fusion, viral entry, HIV-1 RT enzyme activity and cytopathic effects of HIV-1 in a dose-dependent manner [48]. Second one is Diekcol (**6**). Dieckol, eckol, 7-phloroeckol, fucodiphloroethol G and phlorofucofuroeckol phlorotannins exhibited inhibitory effect on SARS CoV 3CLpro activity in a dose-dependent fashion. Among these compounds Dieckol was found to be the most efficient molecule on inhibiting cleavage activity of the 3CLpro enzyme. Docking experiments also supported the important inhibitory effect of Dieckol on SARS CoV 3CLpro enzyme [49]. The last, it shows third good binding affinity value of Phlorofucofuroeckol B (10) toward the target. Interestingly, Kwon HJ et al. reported that, Phlorofucofuroeckol have inhibited Porcine Epidemic Diarrhea Virus PEDV which is belonging to Coronaviridae family of viruses through inhibiting its attachment to the target cell. They also showed that Dieckol, 7-Phloroeckol and Eckol was also had inhibitory effect on virus and target cell attachment. Dieckol, Eckol and Phlorofucofuroeckol displayed strong inhibition of hemaglutination which have been completely blocking virus attachment at intestinal enterocytes. This antiviral activity attributed to a strong interaction with S protein on the outer surface of PEDV which results in restricts the viral adsorption. Dieckol and Phlorofucofuroeckol were found to be have stronger inhibitory effects on the late stage viral replication [50]. However, to our knowledge there is no publication on *in silico* analysis for algal phenolic compounds' binding affinity at ACE2 and TMPRSS2 receptors SARS-COV-2 binding surfaces.

Conclusion

In this study showed that an *in silico* model of algal molecules interactivity on SARS CoV-2-RBD/ACE2 and SARS CoV-2-Spike/TMPRSS2 receptor. In general, computational observations suggests that the hydroxyl group of the related compounds, which are largely responsible for antiviral activities, is a good evidence to refute the existence of current belief. However, to date, no studies have shown an association of the inhibitory effect of these molecules with inflammation of SARS-CoV-2. In summary, this research, based on a broad theoretical approach, can be a guide for future research to learn about molecules selected from algae in the treatment or prevention of SARS-

CoV-2. Pre-clinic studies could be promise as candidate clinical potential in these molecules over SARS – CoV-2 inflammation or different pandemics in future.

Declaration of Interest

The authors declare that the research was conducted in the absence of any commercial or financial relationships that could be construed as a potential conflict of interest.

Data Availability Statement

The datasets generated for this study are available on request to the corresponding authors.

References

1 Holmes EC (2003) Error thresholds and the constraints to RNA virus evolution. Trends Microbiol 11: 543-546.

2 Gallagher TM, Buchmeier MJ (2001) Coronavirus Spike Proteins in Viral Entry and Pathogenesis. Virology 279: 371–374.

3 Li W, Moore MJ, Vasilieva N, Sui J, Wong SK, et al. (2003) Angiotensin-converting enzyme 2 is a functional receptor for the SARS coronavirus. Nature 426: 450–454.

4 Wang T, Jónsdóttir R, Liu H, Gu L, Kristinsson HG, et al. (2012) Antioxidant Capacities of Phlorotannins Extracted from the Brown Algae Fucus vesiculosus. J Agric Food Chem 60: 5874–5883.

5 Glowacka I, Bertram S, Muller MA, Allen P, Soilleux E, et al. (2011) Evidence that TMPRSS2 Activates the Severe Acute Respiratory Syndrome Coronavirus Spike Protein for Membrane Fusion and Reduces Viral Control by the Humoral Immune Response. J Virol 85: 4122–4134.

6 Li F, Li W, Farzan M, Harrison SC (2005) Structure of SARS Coronavirus Spike Receptor-Binding Domain Complexed with Receptor. Science 309: 1864–1868.

7 Röhrig B, Prel JB, Wachtlin D, Kwiecien R, Blettner M (2010) Sample Size Calculation in Clinical Trials. Deutsches Aerzteblatt Online.

8 Pérez M, Falqué E, Domínguez H (2016) Antimicrobial Action of Compounds from Marine Seaweed. Mar Drugs 14: 52.

9 Leyton A, Pezoa-Conte R, Barriga A, Buschmann AH, Maki-Arvela P, et al. (2016) Identification and efficient extraction method of phlorotannins from the brown seaweed Macrocystis pyrifera using an orthogonal experimental design. Algal Res 16: 201–208.

10 Meslet-Cladiere L, Delage L, Leroux CJ, Goulitquer S, Leblanc C, et al. (2013) Structure/Function Analysis of a Type III Polyketide Synthase in the Brown Alga Ectocarpus siliculosus Reveals a Biochemical Pathway in Phlorotannin Monomer Biosynthesis. The Plant Cell 25: 3089–103.

11 Zubia M, Fabre MS, Kerjean V, Lann KL, Stiger-Pouvreau V, et al. (2009) Antioxidant and antitumoural activities of some Phaeophyta from Brittany coasts. Food Chem 116: 693–701.

12 Montero L, Sánchez-Camargo AP, García-Cañas V, Tanniou A, Stiger-Pouvreau V, et al. (2016) Anti-proliferative activity and chemical characterization by comprehensive two-dimensional liquid chromatography coupled to mass spectrometry of phlorotannins from the brown macroalga Sargassum muticum collected on North-Atlantic coasts. J Chromatogr A 1428: 115–125.

13 Gupta S, Abu-Ghannam N (2011) Bioactive potential and possible health effects of edible brown seaweeds. Trends Food Sci Technol 22: 315–326.

14 Li YX, Wijesekara I, Li Y, Kim SK (2011) Phlorotannins as bioactive agents from brown algae. Process Biochem 46: 2219-2224.

15 Ancheeva E, El-Neketi M, Daletos G, Ebrahim W, Song W, et al. (2018) Anti-infective Compounds from Marine Organisms. In P. H. Rampelotto & A. Trincone (Edn), Cham: Springer International Publishing. Grand Challenges in Marine Biotechnology 97-155.

16 Arisawa M, Fujita A, Hayashi T, Hayashi K, Ochiai H, et al. (1990) Cytotoxic and Antiherpetic Activity of Phloroglucinol Derivatives from Mallotus japonicus (Euphorbiaceae). Chem Pharm Bull 38: 1624-1626.

17 Artan M, Li Y, Karadeniz F, Lee SH, Kim MM, et al. (2008) Anti-HIV-1 activity of phloroglucinol derivative, 6,6'-bieckol, from Ecklonia cava. Bioorg Med Chem 16: 7921-7926.

18 Jiménez-Escrig A, Gómez-Ordóñez E, Rupérez P (2011) Seaweed as a Source of Novel Nutraceuticals: Sulfated Polysaccharides and Peptides. In SK. Kim (Ed.). Advances in Food and Nutrition Research Academic Press 64: 325-337.

19 Kim SK, Wijesekara I (2017) Role of Marine Nutraceuticals in Cardiovascular Health. In D. Bagchi (Edn). Sustained Energy for Enhanced Human Functions and Activity. Academic Press 273-279 .

20 Liu Z, Nakamura T, Munemasa S, Murata Y, Nakamura Y (2016) Galloylated Catechins as Potent Inhibitors of Angiotensin Converting Enzyme. Food Sci Technol Res 22: 847-851.

21 Manandhar B, Paudel P, Seong SH, Jung HA, Choi JS (2019) Characterizing Eckol as a Therapeutic Aid: A Systematic Review. Mar Drugs 17: 361.

22 Wright AE, Rueth SA, Cross SS (1991) An antiviral sesquiterpene hydroquinone from the marine sponge Strongylophora hartmani. J Nat Prod 54: 1108-1111.

23 (NCIRD) (2020) Clinical Guidance Management Patients. National Center for Immunization and Respiratory Diseases, Diseases, Division of Viral.

24 Berman HM, Westbrook J, Feng Z, Gilliland G, Bhat TN, et al. (2000) The Protein Data Bank. Nucleic Acids Res 28: 235-242.

25 Berman HM, Henrick K, Nakamura H (2003) Announcing the worldwide Protein Data Bank. Nat Struct Biol 10: 980.

26 Meng T, Cao H, Zhang H, Kang Z, Xu D, et al. (2020) The insert sequence in SARS-CoV-2 enhances spike protein cleavage by TMPRSS. bioRxix.

27 Brooks BR, Bruccoleri RE, Olafson BD, States DJ, Swaminathan S, et al. (1983) A program for macromolecular energy, minimization, and dynamics calculations. J Compt Chem 4: 187-217.

28 Ravindranath PA, Forli S, Goodsell DS, Olson AJ, Sanner MF (2015) Advances in protein-ligand docking with explicitly specified binding site flexibility. PLoS Comput Biol 11: e1004586.

29 Al-Khafaji K, Tok T (2020) Understanding the mechanism of Amygdalin's multifunctional anti-cancer action using computational approach. J Biomol Struct Dyn 1-14.

30 Auto GridFR (AGFR), a free graphical user interface for specifying the docking box. Retrieved from http://adfr.scripps.edu/AutoDockFR/agfr.html

31 Al-Khafaji K, Tok T (2020) Amygdalin as multi-target anticancer drug against targets of cell division cycle: double docking and molecular dynamics simulation. J Biomol Struct Dyn 2: 1-10.

32 Lipinski CA, Lombardo F, Dominy BW, Feeney PJ (2001) Experimental and computational approaches to estimate solubility and permeability in drug discovery and development settings. Adv Drug Deliv Rev 46: 3-26.

33 Veber DF, Johnson SR, Cheng HY, Smith BR, Ward KW, et al. (2002) Molecular properties that influence the oral bioavailability of drug candidates. J Med Chem 45: 2615-2623.

34 Biovia DS (2016) Dassault Systemes BIOVIA, Discovery Studio. San Diego: Dassault Systèmes. Retrieved from https://www.3dsbiovia.com/about/citations-references.

35 Egan WJ, Lauri G (2020) Prediction of intestinal permeability. Adv Drug Deliv Rev 54: 273-289.

36 Oliveira LD, Davi M, Oliveira TD, Mota K (2020) Comparative Computational Study of SARS-CoV-2 Receptors Antagonists from Already Approved Drugs. Chemrxiv 10.

37 Karadeniz FK, Park JW, Park SJ, Kim SK, Egan WJ (2014) Anti-HIV1 activity of phlorotannin derivative 8,4-dieckol from Korean brown alga Ecklonia cava. Biosci Biotechnol Biochem 78: 1151-1158.

38 Egan WJ, Merz KM, Baldwin JJ (2000) Prediction of drug absorption using multivariate statistics. J Med Chem 43: 3867-3877.

39 Jha A, Vimal A, Bakht A, Kumar A (2019) Inhibitors of CPH1-MAP Kinase Pathway: Ascertaining Potential Ligands as Multi-Target Drug Candidate in Candida albicans. Int J Pept Res Ther 25: 997-1010.

40 Dong L, Hu S, Gao J (2020) Discovering drugs to treat coronavirus disease 2019 (COVID-19). Drug Discov Ther 14: 58-60.

41 Shi Q, Wang A, Lu Z, Qin C, Hu J, et al. (2017) Overview on the antiviral activities and mechanisms of marine polysaccharides from seaweeds. Carbohydr Res 453-454: 1–9.

42 COVID-19 Molecular Structure and Therapeutics Hub. Retrieved from https://COVİD.bioexcel.eu/. 2020.

43 Kong R, Wang F, Zhang J, Wang F, Chang S, et al. (2019) A Multistage Approach for Global and Site-Specific Protein-Protein Docking. J Chem Inf Model. 59: 3556-3564.

44 Kong R, Yang G, Xue R, Liu M, Wang F, et al. (2020) COVID-19 Docking Server: An interactive server for docking small molecules, peptides and antibodies against potential targets of COVID-19. Bioinformatics.

45 Trott O, Olson AJ, Vina AD (2010) Improving the speed and accuracy of docking with a new scoring function, efficient optimization and multithreading. J Comput Chem 31: 455-461.

46 Weis WI, Drickamer K (1996) Structural Basis of Lectin-Carbohydrate Recognition. Annual Rev 65: 441-473.

47 Lung J, Lin YS, Yang YH, Chou YL, Shu LH, et al. (2020) The potential chemical structure of anti-SARS-CoV-2 RNA-dependent RNA polymerase. Journal of medical virology 92: 693-697.

48 Artan M, Li Y, Karadeniz F, Lee SH, Kim MM, et al. (2008) Anti-HIV-1 activity of phloroglucinol derivative, 6,6'-bieckol, from Ecklonia cava. Bioorg Med Chem 16: 7921-7926.

49 Kang KA, Lee KH, Park JW, Lee NH, Na HK, et al. (2007) Triphlorethol-A induces heme oxygenase-1 via activation of ERK and NF-E2 related factor 2 transcription factor. FEBS Lett 581: 2000-2008.

50 Kwon HJ, Ryu YB, Kim YM, Song N, Kim CY, et al. (2013) In vitro antiviral activity of phlorotannins isolated from Ecklonia cava against porcine epidemic diarrhea coronavirus infection and hemagglutination. Bioorg Med Chem 21: 4706-4713.